

Proton dynamics in $\text{Cs}_2(\text{HSO}_4)(\text{H}_2\text{PO}_4)$ studied by ^1H NMR

Shigenobu Hayashi*, Masagi Mizuno

Research Institute of Instrumentation Frontier, National Institute of Advanced Industrial Science and Technology (AIST), Tsukuba Central 5, 1-1-1 Higashi, Tsukuba, Ibaraki 305-8565, Japan

Received 7 July 2004; received in revised form 5 October 2004; accepted 14 October 2004

Abstract

Proton dynamics in $\text{Cs}_2(\text{HSO}_4)(\text{H}_2\text{PO}_4)$ has been studied by ^1H NMR. The compound shows a large thermal history. The high-temperature phase (phase HT) is retained for a considerably long period on cooling. The original room-temperature phase (phase RT) does not recover on cooling from phase HT, and another room-temperature phase (phase RT2) is produced. ^1H NMR spectra indicate that reorientation of the SO_4/PO_4 tetrahedron takes place in phases RT and RT2 and that protons diffuse translationally in phases RT2 and HT. In all the phases, the mean residence time of protons has a distribution, being demonstrated by ^1H spectral line shapes and ^1H spin-lattice relaxation times. Protons diffuse with the inverse of the frequency factor (τ_0) of 0.90×10^{-13} s and the activation energy (E_a) of 36 kJ/mol in phase HT, being obtained from analysis of the ^1H spin-lattice relaxation times. These parameters can well explain the macroscopic electric conductivity. Reorientation of the SO_4/PO_4 tetrahedron limits the proton transport in phase HT as well as in phase RT2.

© 2004 Elsevier B.V. All rights reserved.

PACS classification: 66.30.Hs; 76.60.Es

Keywords: Proton dynamics; Proton conduction; Inorganic solid acid; Nuclear magnetic resonance; NMR; Spin-lattice relaxation

1. Introduction

Fuel cells are very attractive for electrical power generation because of their high efficiency in energy conversion and low pollution levels. Among them, polymer electrolyte membrane fuel cells are suitable for transportation systems and mobile uses. However, polymer electrolyte membranes require humid atmospheres, which limits the operating temperature to lower than 373 K. To circumvent the above limitation, Haile et al. [1,2] used inorganic solid acids such as CsHSO_4 and CsH_2PO_4 as the electrolytes, and demonstrated that inorganic, water-soluble solid acids are used successfully in H_2/O_2 and direct methanol fuel cells.

It is well known that a high proton conductivity is observed in a high-temperature phase, so-called “a superprotonic phase”, of solid acids such as $\text{MH}(\text{AO}_4)$ and

$\text{M}_3\text{H}(\text{AO}_4)_2$ ($\text{M}=\text{Cs}, \text{NH}_4, \text{Rb}$; $\text{A}=\text{S}, \text{Se}$) [3–6]. In these compounds tetrahedral AO_4 anions form hydrogen bond networks. It has been presumed that the proton transport takes place through the hydrogen bond, being mediated by reorientation of the AO_4 tetrahedron.

Among the solid acids, CsHSO_4 is the most basic and has been studied extensively. There are several phases depending on temperature and pressure [7], and their crystal structures have already been studied [7–11]. Solid-state NMR is suitable to study proton dynamics at molecular levels. A few reports have already been published on CsHSO_4 [12–15]. We have also studied proton dynamics in this substance previously [16,17].

The superprotonic phase was also observed in phosphates such as MH_2PO_4 ($\text{M}=\text{Cs}, \text{Rb}$) [18,19]. The use of pressure or elevated water partial pressure was required to stabilize the superprotonic phase. Yamada et al. [20] have demonstrated the PO_4 reorientation in the paraelectric phase of CsH_2PO_4 by ^1H and ^{31}P solid-state NMR.

The complex system of $\text{CsHSO}_4\text{--CsH}_2\text{PO}_4$ shows high electric conductivity [21–23] and the structure has been

* Corresponding author. Tel.: +81 29 861 4515; fax: +81 29 861 4515.

E-mail address: hayashi.s@aist.go.jp (S. Hayashi).

studied [24]. The presence of the superprotonic phase was demonstrated in $\text{Cs}_3(\text{HSO}_4)_2(\text{H}_2\text{PO}_4)$, $\beta\text{-Cs}_3(\text{HSO}_4)_2(\text{H}_x(\text{P,S})\text{O}_4)$ and $\text{Cs}_2(\text{HSO}_4)(\text{H}_2\text{PO}_4)$ [21–23]. However, the mechanism of proton diffusion has not been studied so far.

In the present work, we have studied proton dynamics in $\text{Cs}_2(\text{HSO}_4)(\text{H}_2\text{PO}_4)$ by means of ^1H solid-state NMR. We have measured and analyzed ^1H spectral line shapes and spin-lattice relaxation times. We also present high-resolution solid-state NMR spectra of ^1H and ^{31}P . We discuss the mechanism of proton transport; the roles of the reorientation of the SO_4/PO_4 tetrahedron and the proton transfer between two tetrahedra along a hydrogen bond.

2. Experimental

2.1. Materials

Cesium sulfate (Cs_2SO_4 , 99.9%) and phosphoric acid (H_3PO_4 , 85%) were obtained from Junsei Chemical (Tokyo) and Wako Pure Chemical Industries (Osaka), respectively. Equimolar amounts of Cs_2SO_4 and H_3PO_4 were dissolved in a small amount of water. After the solution was concentrated by evaporation under a flow of warm air, it was kept at room temperature. The precipitated crystalline solid was separated by filtration, washed by a small amount of ethanol and then dried in a vacuum desiccator under a reduced pressure.

2.2. X-ray powder diffraction and thermal analyses

X-ray powder diffraction patterns were measured by a Rigaku MiniFlex diffractometer with $\text{Cu K}\alpha$ radiation at room temperature.

Thermogravimetric and differential thermal analyses (TG-DTA) were performed by a Rigaku ThermoFlex TG 8110 combined with a Rigaku thermal analysis station TAS100 in air. The temperature was increased at a rate of 10 K/min from room temperature to 523 K.

Differential scanning calorimetry (DSC) was measured by a Rigaku Thermo Plus DSC 8230 in a N_2 atmosphere. The sample temperature was increased and decreased repeatedly at a rate of 5 K/min.

2.3. NMR measurements

The NMR measurements at 200.13 MHz were performed using a Bruker ASX200 spectrometer with a static magnetic field strength of 4.7 T. A Bruker broadband probehead with a solenoid coil was used to measure ^1H spectra and spin-lattice relaxation times, T_1 , for a static sample. The solid echo pulse sequence ($90^\circ_x-\tau_1-90^\circ_y-\tau_2$ -echo) was used to trace the spectra and the latter half of the echo signal was Fourier-transformed. The saturation recovery pulse

sequence followed by the solid echo pulse sequence [$(90^\circ-\tau_3)_n-\tau-90^\circ_x-\tau_1-90^\circ_y-\tau_2$ -echo] was used for the measurements of spin-lattice relaxation times. The τ value denotes the variable delay time and τ_1 , τ_2 and τ_3 are fixed delay times. The sample temperature was changed between 240 and 495 K with errors less than 2.0 K. The frequency scale of the spectra is expressed with respect to neat tetramethylsilane.

The ^1H spin-lattice relaxation times were also measured by Bruker Minispec mq20 operating at 19.65 MHz. The sample temperature was changed between 230 and 493 K. The inversion recovery pulse sequence ($180^\circ-\tau-90^\circ$) and the saturation recovery ($90^\circ-\tau-90^\circ$) pulse sequence were used, where τ denotes the variable delay time.

The ^1H and ^{31}P magic-angle-spinning (MAS) NMR spectra were measured by a Bruker ASX400 spectrometer with a static magnetic field strength of 9.4 T. Larmor frequencies of ^1H and ^{31}P were 400.13 and 161.98 MHz, respectively. A Bruker MAS probehead was used with a 4-mm zirconia rotor. The frequency scales of the spectra of ^1H and ^{31}P were expressed with respect to neat tetramethylsilane (TMS) by adjusting the signal of adamantane spinning at 8 kHz to 1.87 ppm and with respect to 85% H_3PO_4 aqueous solution by adjusting the signal of $(\text{NH}_4)_2\text{HPO}_4$ to 1.33 ppm, respectively.

3. Results and discussion

3.1. X-ray powder diffraction and thermal analyses

The X-ray powder diffraction pattern of the as-prepared sample agrees very well with literature data [24] as well as with the calculated pattern using the crystal structure in Ref. [24], as shown in Fig. 1. Thus, we confirm that the

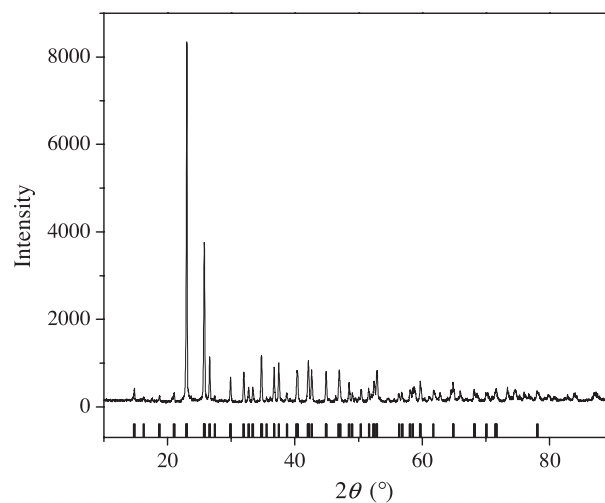


Fig. 1. The X-ray powder diffraction pattern of the as-prepared sample. Bars at the bottom are calculated peak positions for the crystal structure of phase RT in Ref. [24].

Download English Version:

<https://daneshyari.com/en/article/9761729>

Download Persian Version:

<https://daneshyari.com/article/9761729>

[Daneshyari.com](https://daneshyari.com)